Technical Document

Draft 1.0

Q^2 Determination for the Backward Running Phase of the G^0 Experiment

J. M. Mammei*

Virginia Tech

Contents

1 Introduction **4**

2 Q^2 Determination **4**

2.1 Sensitivity Study 5

2.2 Radiative Effects 6

2.3 Q^2 for Measured Beam Energies 7

3 Summary and Conclusions **8**

A Sensitivity Study Plots **9**

B Measured Beam Energies **14**

List of Figures

1 Q^2 as a function of a shift in energy for LH2 362MeV. 5

2 Comparing "unradiated" and "tree level, radiated" Q^2. 7

3 Q^2 as a function of a shift in z of the detectors for all target/energy combinations. 9

4 Q^2 as a function of a shift in radial position of the detectors for all target/energy combinations. 10

5 Q^2 as a function of a shift in target z position for all target/energy combinations. 11

6 Q^2 as a function of a shift in energy for all target/energy combinations. . . . 12

7 Q^2 as a function of a shift in magnetic field for all target/energy combinations. 13

8 Energy from run starts vs. run number with measured energy at approximate time in March 2006. 14

9 Energy from run starts vs. run number with measured energy at approximate time in the summer '06. 14

10 Energy from run starts vs. run number with measured energy at approximate time in September 2006. 15

11 Energy from run starts vs. run number with measured energy at approximate time in December 2006. 15

12 Energy from run starts vs. run number with measured energy at approximate time in winter '07. 16

13 Energy from run starts vs. run number with measured energy at approximate time in March 2007. 16

List of Tables

1 Q^2 sensitivities assuming $\frac{\Delta Q^2}{Q^2} = 1\%$. 6

2 Q^2 Summary; errors include 0.4% model uncertainty (section 2.2). 8

1 Introduction

This document describes the method for estimating the Q^2 and the uncertainties from simulation and the measured energies for the various run periods in the backward angle phase of the G^0 Experiment. The quoted precision for the G^0 backward angle Q^2 was 1% (see Table 6.1 in [1]). The physics asymmetry is proportional to Q^2:

$$A = [\frac{-G_F Q^2}{4\sqrt{2}\pi\alpha}]\frac{\epsilon G_E^\gamma G_E^Z + \tau G_M^\gamma G_M^Z - (1 - 4sin^2\theta_W)\epsilon' G_M^\gamma G_A^e}{\epsilon(G_E^\gamma)^2 + \tau(G_M^\gamma)^2} \tag{1}$$

and each of the form factors is a function of Q^2, so it is important to know the value of this quantity and understand the uncertainty in our experiment. In the forward angle it was possible to determine the Q^2 using time-of-flight information (see [2] for a description) but that is not possible in the backward angle.

2 Q^2 Determination

In the backward angle we detect the elastically scattered electrons. Q^2 is a function of the incident energy E, the scattered electron energy E' and the scattering angle θ

$$Q^2 = 4EE' sin^2\frac{\theta}{2} \tag{2}$$

Because we are primarily interested in elastic scattering, the scattered energy and angle are related by

$$E' = \frac{E}{1 + \frac{2E}{M_p} sin^2\frac{\theta}{2}} \tag{3}$$

where M_p is the mass of the proton. So the Q^2 can be written as a function of incident energy and scattering angle

$$Q^2 = \frac{4E^2 sin^2\frac{\theta}{2}}{1 + \frac{2E}{M_p} sin^2\frac{\theta}{2}} \tag{4}$$

Essentially the Q^2 is a function of the incident energy and the scattering angle which is defined by the acceptance of the collimators, magnetic field and detectors.

The determination of Q^2 then comes from understanding the acceptances in the experiment. This was done by verifying the positions of the target, collimators and detectors relative to each other in the simulation using hall surveys. In addition, the properly radiated yields from simulation do a fairly good job of reproducing the measured yields, so this gives us some confidence that we understand the acceptance of the experiment.

2.1 Sensitivity Study

In order to gauge the effects of uncertainties in detector and target position, as well as beam energy and magnetic field, a sensitivity study was performed in simulation. For each quantity the locus average Q^2 was calculated for shifts from the nominal value of the quantity, and plots were made of the Q^2 vs. the shifts (See Figure 1). All of the plots from the study are shown in the appendix A. The data were fit with a line and the slope of the line $\frac{\partial Q^2}{\partial x}$ was used to calculate the sensitivity to that quantity assuming that $\frac{\Delta Q^2}{Q^2} = 1\%$ (see Table 1). The units are given by the expected uncertainties, which are shown in the last column. The sensitivities to the various quantities are all much smaller than the expected uncertainties in the various quantities, except for the beam energy. The expected uncertainty in the beam energy is close to the sensitivity in Q^2; this number was estimated using the errors on the measured beam energies (see Table 2). The spread in the energies from the run starts is smaller, but the central value is different from the measured energies by almost 1 MeV (see appendix B).

Figure 1: Q^2 as a function of a shift in energy for LH2 362MeV.

The effect of a radial shift is perhaps easiest to understand. A negative shift in radius moves the detectors closer to the beamline, thus causing the acceptance to change to higher Q^2, because we are looking at backward angle scattering where the higher angle is at a lower radius. So the slope of the Q^2 with radial shift is negative. A negative shift in the z position

Table 1: Q^2 sensitivities assuming $\frac{\Delta Q^2}{Q^2} = 1\%$.

x	**362 LH2**	**362 LD2**	**687 LH2**	**687 LD2**	Δx
z_{det}	19	18	23	10	1.0cm
r_{det}	5	3	8	5	0.5cm
z_{tar}	5	4	10	6	0.5cm
E_{beam}	2	2	4	5	1.0MeV
$BFIL$	6	23	7	16	1.3%

of the detectors moves them closer to the target, which is like a shift to higher radius, so the slope of the Q^2 with a shift in z should be positive. A negative shift in target position moves the target upstream. Roughly this should be like moving to a larger radius, or a lower Q^2, so the slope of the Q^2 vs. target shift should be positive. This is not exactly what is happening because the scattered electrons also experience a different field. A shift in magnet current would be proportional to a shift in the field. This would change the radial position of the rays as they exit the collimators. A lower field would be like moving the detectors to a lower radius, or higher Q^2. So the slope of the magnetic field plots should be negative. Shifting the beam energy should result in a postive slope (Eq. 4). The measured beam energies will be discussed further in section 2.3.

One thing to note is that the nominal Q^2 is about 1% lower in the sensitivity plots than the quoted numbers. This is because the simulations for the study were run with the incorrect eloss. This will be discussed in more detail in section 2.2. It is assumed that the slope of the plots would be unaffected.

2.2 Radiative Effects

The radiative correction will be applied to the asymmetries and not to the yields. This brings up the question of how to get the "unradiated" Q^2 from the simulation. If one uses a simulation with no radiative effects, then the yield distribution will not be the same as that of the experiment. So one could, in principle, use the "tree level" Q^2 from a fully radiated simulation, where the yield distribution would be more similar to that of the experimental

yields, so the averaging over the locus would be more similar. It turns out that the difference between the Q^2 in these two cases is about 0.4%. The proposal is to use the "unradiated" Q^2 with an error bar of 0.4% to make it consistent with the "tree level" Q^2 from a fully radiated simulation. These are the numbers reported in Table 2.

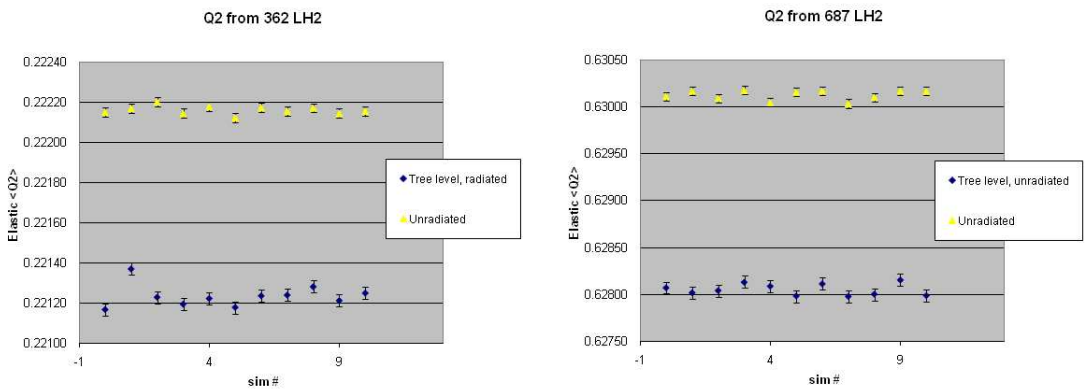

Figure 2: Comparing "unradiated" and "tree level, radiated" Q^2.

The "unradiated" Q^2 was obtained by performing a simulation using eloss_rad with IRADE, IRADI and IIONI set to zero, which has the energy loss before the scattering vertex, but turns off the radiative effects. The "tree level" Q^2 was obtained by using the full radiative correction but calculating the Q^2 from the pre-radiated angle and scattered electron energy.

2.3 Q^2 for Measured Beam Energies

In order to estimate the Q^2 for the measured beam energies, a Taylor expansion around the nominal values was used.

$$Q^2(E) = Q^2(E_o) + \frac{\Delta Q^2}{\Delta E}(E - E_o) \tag{5}$$

The simulation nominal beam energies are 687MeV and 362MeV and the Q^2 values are 0.6301 $\frac{GeV^2}{c^2}$ and 0.2222 $\frac{GeV^2}{c^2}$ respectively. For the high energy running periods the energy was measured by Mark Jones using the Hall C method. For the low energies Hall A provided a measurement for the Summer '06 run period based on the two spectrometer arms. They were unable to performs this analysis for the Winter '07 run period, so that energy was obtained by scaling by the ratio of the of the energies from the run starts for the two periods (see Figures 12 and 9). The uncertainty on the Winter '07 energy reflects the error due to this scaling.

Table 2: Q^2 Summary; errors include 0.4% model uncertainty (section 2.2).

Run Period / Date	**Target / Energy**	**Systematic Error (%)**	**Beam Energy (MeV)**	**Energy (MeV)**	**Q^2 ($\frac{GeV^2}{c^2}$)**
April 17, 2006	LH2 / 687	0.21	685.57 ± 0.92	682.45 ± 0.92	0.6275 ± 0.003
Summer 2006	LH2 / 362	0.27	361.90 ± 0.50	358.75 ± 0.50	0.2217 ± 0.001
Sept. 27,2006	LH2 / 687	0.27	684.86 ± 0.92	681.74 ± 0.92	0.6264 ± 0.003
Dec. 19, 2006	LD2 / 687 (M2)	0.19	689.61 ± 0.93	686.07 ± 0.93	0.6300 ± 0.003
Dec. 19, 2006	LD2 / 687 (M3)	0.19	689.61 ± 0.93	686.05 ± 0.93	0.6287 ± 0.003
Winter 2007	LD2 / 362	0.22	363.05 ± 0.66	359.51 ± 0.66	0.2193 ± 0.001
March 14, 2007	LD2 / 687	0.19	689.42 ± 0.93	686.87 ± 0.93	0.6299 ± 0.003

3 Summary and Conclusions

The final numbers for the mean Q^2, center of target energies and uncertainties are presented in Table 2. The Q^2 and energy values come from simulations at the beam energies. The additional uncertainty in the "center of target" energy that comes from the error on the energy loss is negligible. The uncertainty on the Q^2 does not include the systematic uncertainty from an energy variation; but does include a systematic uncertainty that includes the Δx numbers reported in the last column in Table 1.

A Sensitivity Study Plots

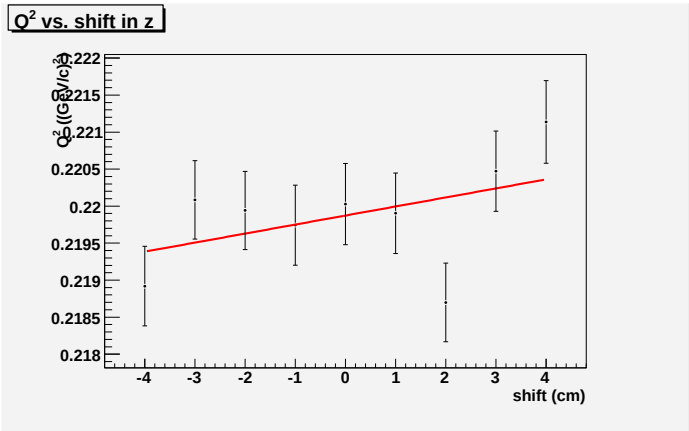

LD2 362

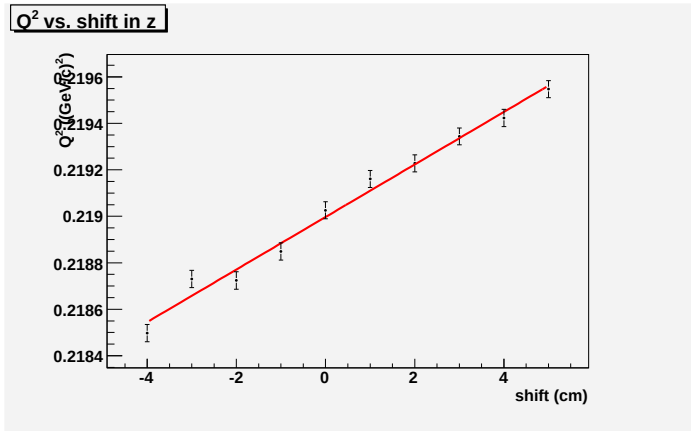

LH2 362

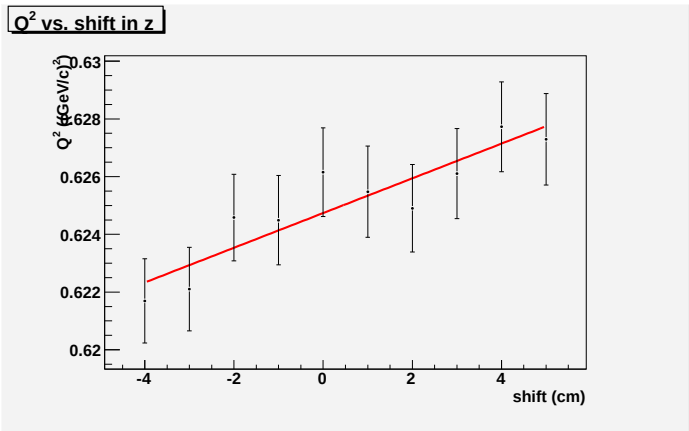

LD2 687

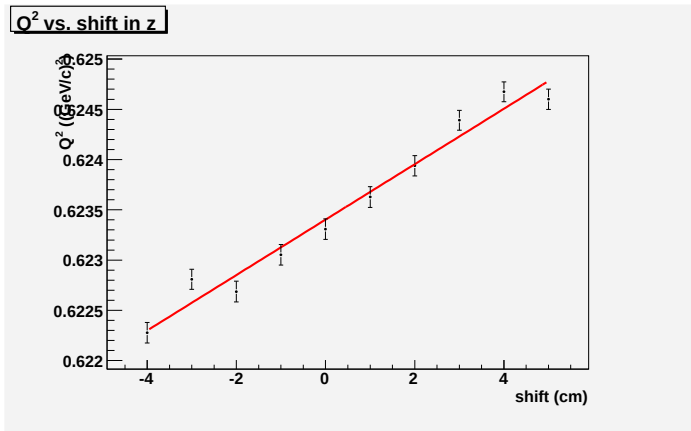

LH2 687

Figure 3: Q^2 as a function of a shift in z of the detectors for all target/energy combinations.

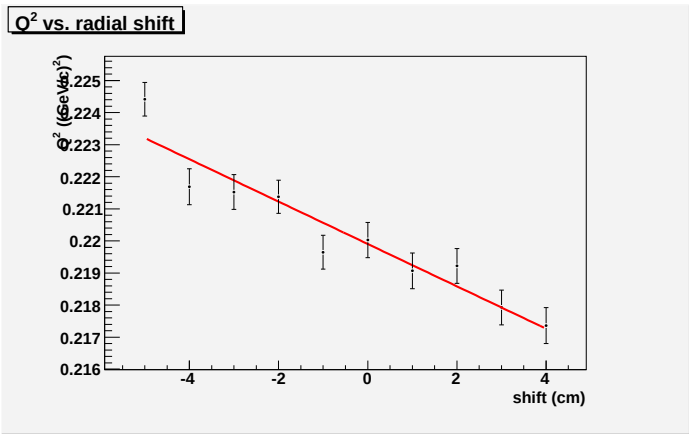

LD2 362

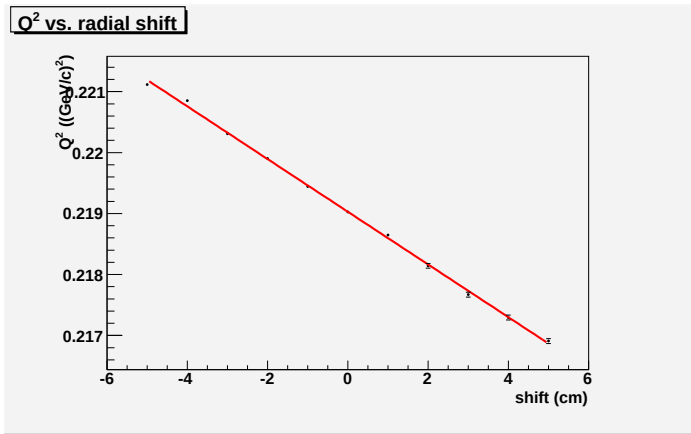

LH2 362

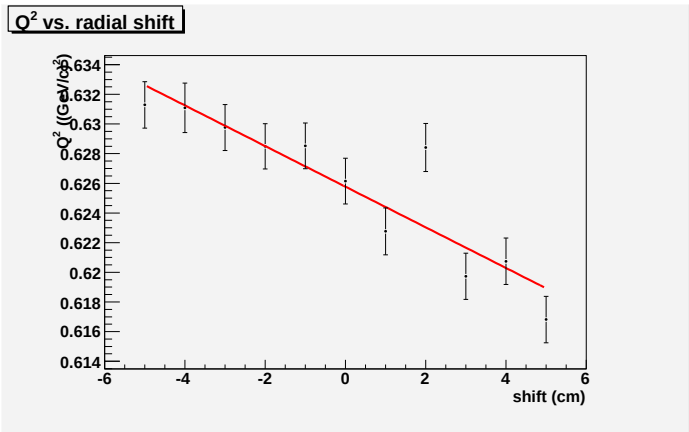

LD2 687

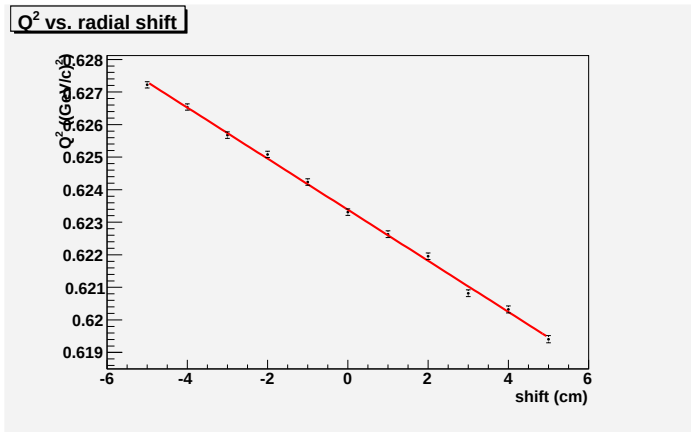

LH2 687

Figure 4: Q^2 as a function of a shift in radial position of the detectors for all target/energy combinations.

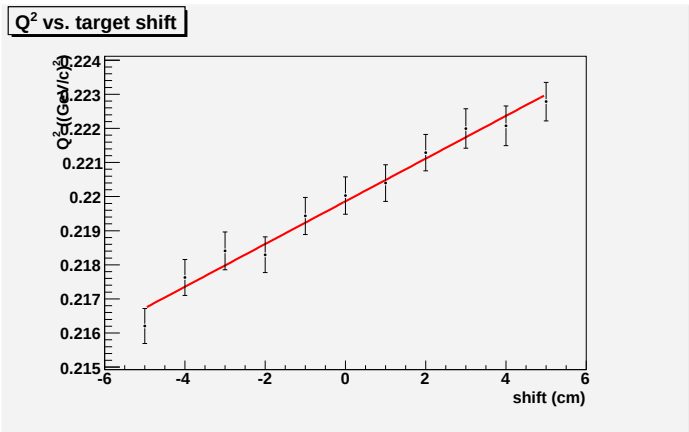

LD2 362

LH2 362

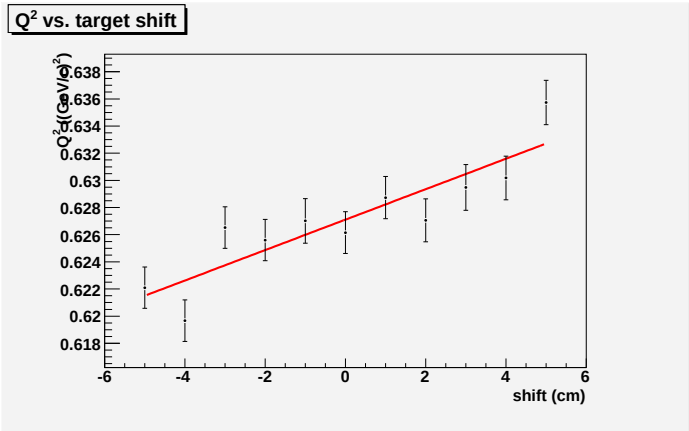

LD2 687

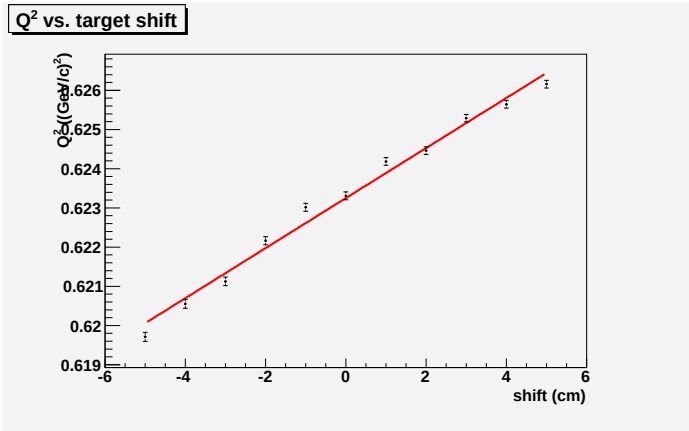

LH2 687

Figure 5: Q^2 as a function of a shift in target z position for all target/energy combinations.

LD2 362

LH2 362

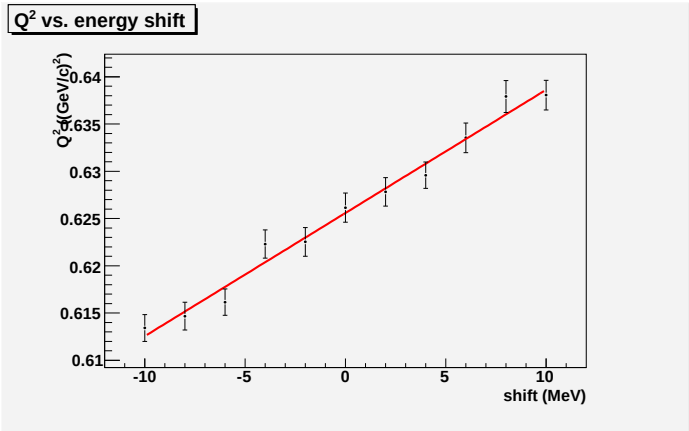

LD2 687

LH2 687

Figure 6: Q^2 as a function of a shift in energy for all target/energy combinations.

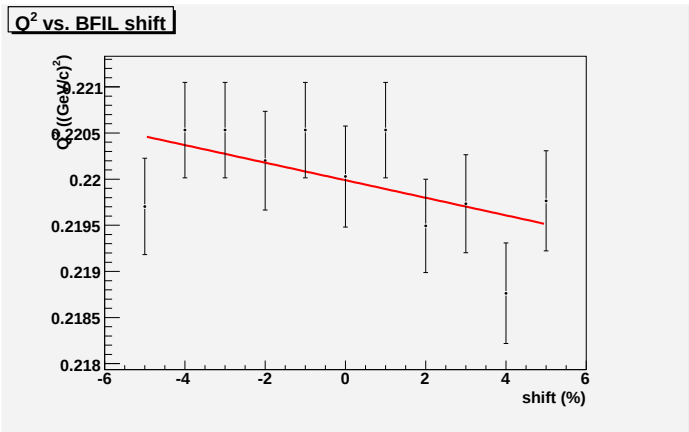

LD2 362

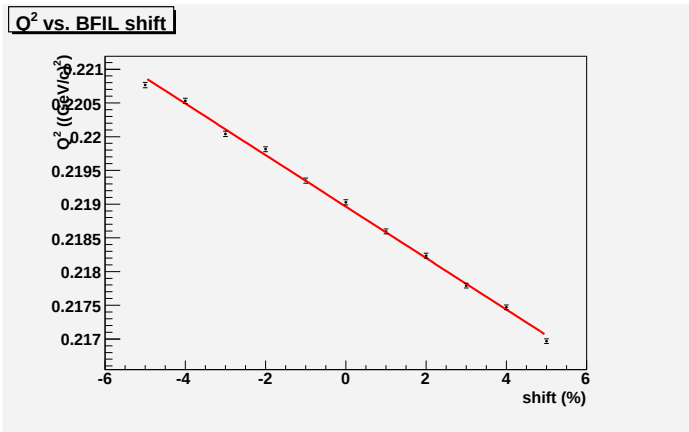

LH2 362

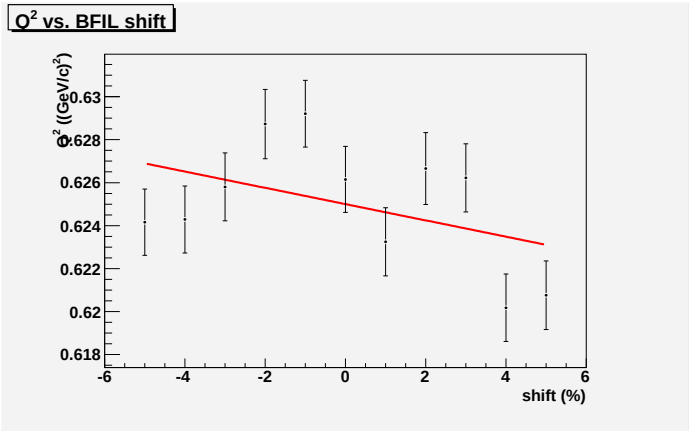

LD2 687

LH2 687

Figure 7: Q^2 as a function of a shift in magnetic field for all target/energy combinations.

B Measured Beam Energies

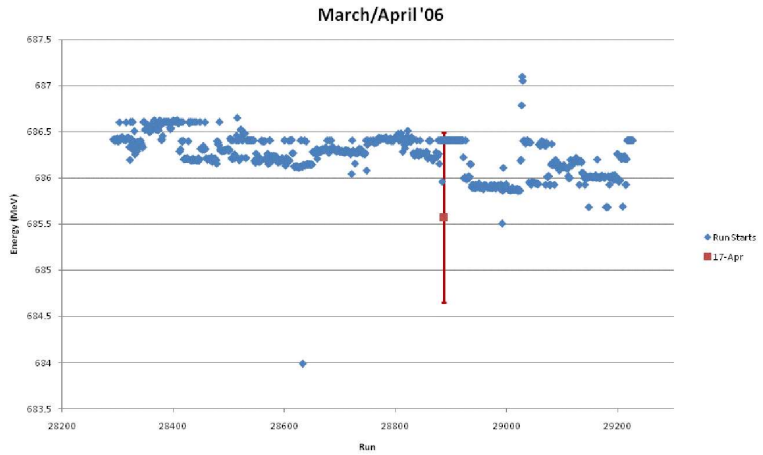

Figure 8: Energy from run starts vs. run number with measured energy at approximate time in March 2006.

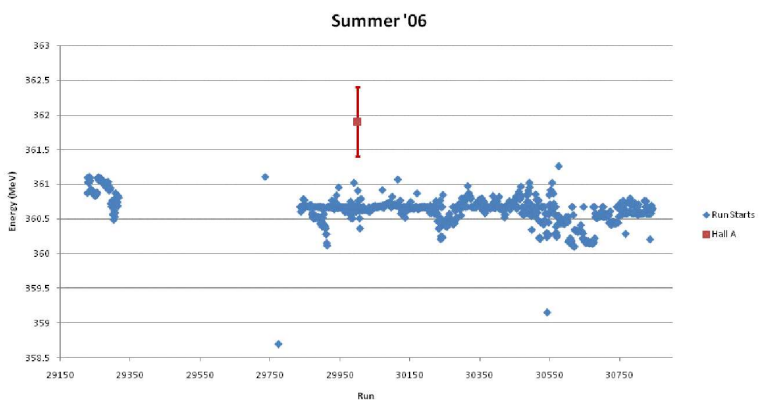

Figure 9: Energy from run starts vs. run number with measured energy at approximate time in the summer '06.

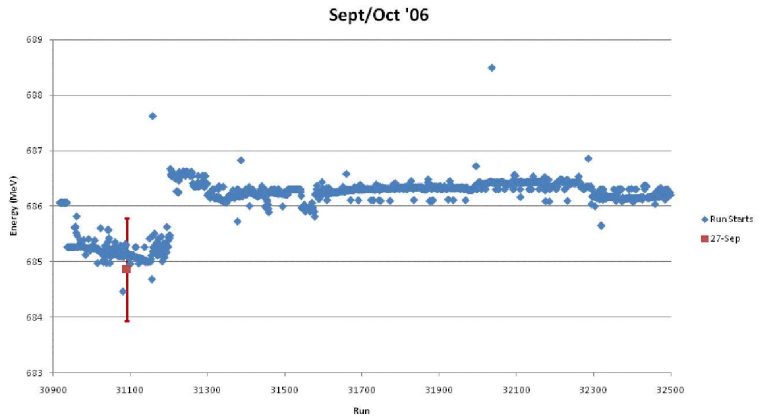

Figure 10: Energy from run starts vs. run number with measured energy at approximate time in September 2006.

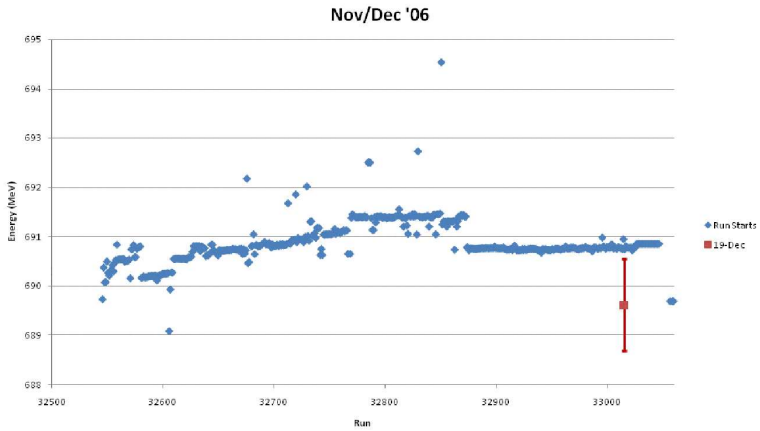

Figure 11: Energy from run starts vs. run number with measured energy at approximate time in December 2006.

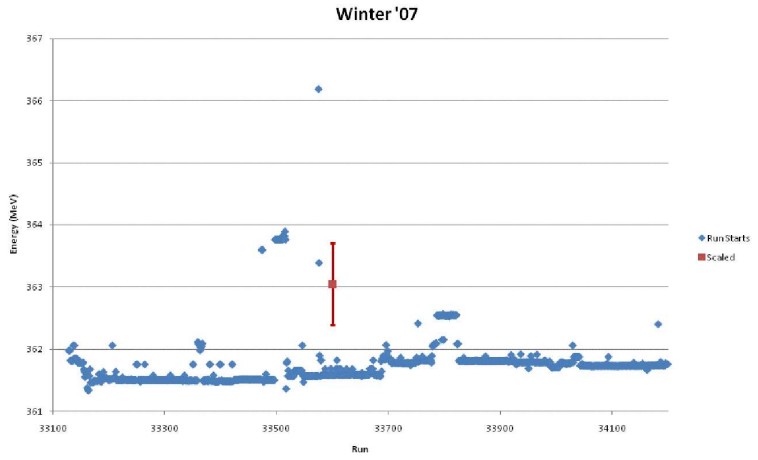

Figure 12: Energy from run starts vs. run number with measured energy at approximate time in winter '07.

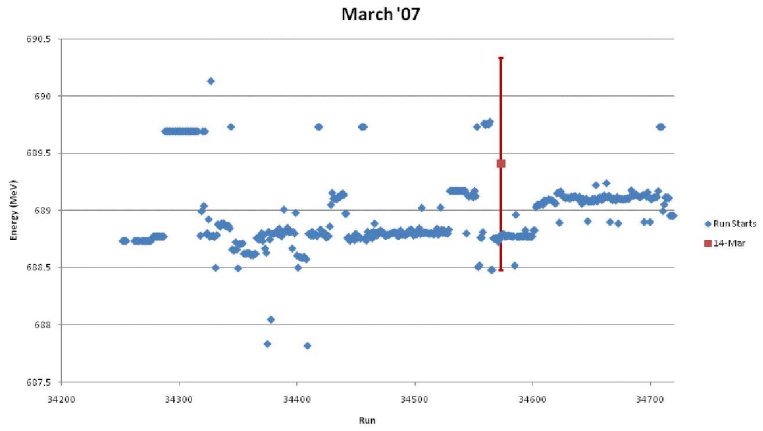

Figure 13: Energy from run starts vs. run number with measured energy at approximate time in March 2007.

References

[1] The G^0 Experiment Backward Angle Measurements Update. The G^0 Collaboration. June 2005.

[2] Q^2 determination in the G^0 Experiment. G^0 France. Gilles Que'me'ner.